Date of publication December 1, 2023.

Simulation and calculation of wide frequency harmonic temperature rise based on dry type hollow reactor

WANWEI WANG[1], RAN ZHUO[2], RONGFU ZHONG[1], ZHIMING HUANG[2], CHENGZHOU ZHANG[1], YAN LUO[2], JIEMING HUANG[1], MENG GAO[2], QIULIN CHEN[2], AND YUN ZHANG[2]

[1]The State Key Laboratory for Management and Control of Complex Systems, Institute of Automation, Chinese Academy of Sciences, Beijing 100190, China
[2]The Macao Institute of Systems Engineering, Macau University of Science and Technology, Macao 999078, China
[1]Honors School, Monmouth University, W. Long Branch, New Jersey, USA
[2]Department of Computer Science and Software Engineering, Monmouth University, W. Long Branch, New Jersey, USA.
[1]Dongguan bureau of power supply, Guangdong power grid CO.LTD, Dongguan, China
[2]High Voltage Research Department, CSG Electric Power Research Institute CO.,LTD, Guangzhou, China

Corresponding author: Yan Luo (e-mail: luoyan1009@yeah.net).

This work is supported by science and technology project of Guangdong Power Grid Corporation (031900KK52210023(GDKJXM20210092)).

ABSTRACT With the increasing size of the grid, a large number of non-linear equipment applicable, harmonic pollution is becoming more and more serious. Higher demands on the harmonic operation capability of reactor filtering equipment. In this paper, the dry type hollow reactor was taken as a research object, according to the field-circuit coupling principle, the establishment of finite element two-dimensional wire-turn unit electromagnetic simulation calculation model, solved the coil frequency current superimposed on different harmonic current frequency, content curve. Then calculate the winding loss of each layer, carry out the fluid-heat coupling simulation calculation, and get the temperature rise distribution of the reactor. Study shows that: Elevated harmonic content causes an increase in coil current amplitude and excitation of a stronger magnetic field, resulting in an increase in resistance loss and eddy current loss, leading to a rise in reactor temperature. The increase in harmonic frequency marginalizes the reactor coil current density distribution, increases the coil resistance, and leads to an increase in the local magnetic induction strength, resulting in an increase in coil eddy current losses, leading to an increase in reactor temperature.

INDEX TERMS Dry type hollow reactor, harmonics, Coil Loss, Temperature rise calculation.

I. INTRODUCTION

In recent years, with the strategic goal of "carbon peak-carbon neutral", the safe, efficient, green and low-carbon transformation of energy and power systems has become a global development trend [1-3], and a large number of new clean energy sources, such as solar energy, wind energy, tidal energy, etc., are added to the power grid system through non-linear devices [4], resulting in a decrease in the harmonic content of the system at the 3rd, 5th and 7th harmonics , which poses a new challenge to the power quality of the power system. 7th harmonic content has all declined, generating broadband harmonics with higher frequency and content from 7th to 70th [5-6], which poses a new challenge to the power quality of the power system. Series reactors can effectively limit the high harmonics in the system. However, the dry type hollow reactor has serious magnetic leakage compared to the traditional oil-immersed iron core reactor, which will generate eddy currents in the surrounding magnetically conductive equipment and cause unnecessary losses, and according to the static magnetic field exposure guidelines developed by the ICNIRP [7], the static magnetic field exposure limit for the general public is 400 mT, and the exposure limit for the occupational personnel's head and torso, and the limbs is 2T and 4T, respectively. However, this year in the practical application, the hollow reactor has been used in a wide range of applications, and is prone to local discharge [8], overheating burnout [9] and other faults during operation. Therefore, it is of great significance to establish the electromagnetic simulation model of dry-type hollow reactor, and analyze the influence of broadband electromagnetic parameters and temperature rise on the reactor failure prevention, design and improvement.

A. RELATED WORKS

At present, domestic scholars have done a lot of research on the temperature field of dry-type air-core reactor. Literature [10] investigated the electromagnetic calculations and losses of dry type air-core reactors, proposing the isothermal rise method as a design method and using the Bartky transform method to accurately calculate the magnetic induction intensity in the reactor winding space. Literature [11] Improvement of the ventilation structure of dry hollow reactor by coupled field numerical calculation method effectively reduces the local temperature rise and improves the heat dissipation performance and operation safety of the reactor. Literature [12] simulated the temperature rise of the reactor by means of a multi-physical field coupling method and verifies its accuracy. Literature[13] analyzed the temperature field distribution and hot spot temperature rise of the reactor by using the finite element method with the steady-state temperature field as an example; domestic scholars, Prof. Wei Xinlao, deduced the analytical formula of the encapsulation loss, and further deduced the analytical formula of the encapsulation temperature rise based on the principle of equal current density[14], and scholars, Zhao Haixiang, used the curve-fitting method combined with the heat balance formula to derive the calculation of the average temperature rise of the encapsulation[15], Xia Wei and other scholars used a hybrid calculation method to calculate and analyze the eddy current loss of dry-type hollow reactor [16], established the partial differential equation of the temperature field of dry-type hollow reactor, combined with the natural convection coefficient formula of heat transfer, and analytically calculated the temperature distribution of the reactor [17]. Ye Zhanguang conducted relevant studies on the temperature rise test, the temperature rise of encapsulated hot spots and the average temperature rise of dry-type hollow reactors [18]. Scholars such as Zhang Liangxian and Zeng Linliao proposed to use the loss separation method to study the loss of extra-high voltage dry flat wave reactors [19]. Deng Qiu, Li Zhenbiao and other scholars simulated the flow field and temperature field of a five-layer encapsulated dry hollow reactor based on the fluid-solid coupling approach, and investigated the relationship between the air flow velocity and the hot spot temperature under forced convection [20]. Foreign scholars have carried out more research on reactor losses, P.E. Burke and other scholars proposed the use of impedance matrix to calculate the encapsulated eddy current loss of dry-type hollow reactor, which provides a basis for the design of dry-type hollow reactor [21].B.S. Sam and other scholars have carried out a study on the inductance and encapsulated eddy current loss of dry-type hollow reactor [22]. Naoyuki Kurita and other scholars have studied the inductance of amorphous iron core three-phase AC reactor and temperature field of the dry-type air-core three-phase AC reactor and simulated the relationship between air velocity and hot spot temperature under forced convection [20]. The eddy current loss of three-phase AC reactor with amorphous core was calculated and analyzed by using finite element method in conjunction with B-H curves for encapsulated toroidal design and encapsulated sectoral design [23]. Carlos Ortiz et al. analyzed the conjugate heat transfer problem of dry-type transformer under natural cooling conditions based on computational fluid dynamics combined with parallel computation [24]. To summarize the literature, only the accuracy of simulation and calculation of reactor operability at the rated frequency of the system is investigated, and the detailed analysis and study of the system under mixed complex frequency harmonic conditions is missing.

B. OUR WORK

In this paper, a 35kV dry type hollow reactor is used as the object of temperature rise study, firstly, according to its physical and electrical structure, a two-dimensional wire-turn unit electromagnetic simulation model based on ANSYS-MAXWELL is established, and a three-dimensional 1/4 reactor current and heat simulation model based on Comsol as well as an equivalent circuit is established. Then the two-dimensional electromagnetic field and circuit coupling calculation is carried out to solve the fundamental current and integrate the harmonic current solution to obtain the total current curve. The fusion current curves with different harmonic current frequencies and contents are used as the excitation to solve the magnetic induction intensity distribution and reactor coil loss, and finally the temperature rise distribution is obtained by the reactor multi-physical field coupling calculation according to the flow-heat principle, which provides a reference for the design of reactor fault prevention under harmonic conditions.

II. REACTOR STRUCTURE AND SIMULATION MODELING

A. REACTOR STRUCTURE PARAMETERS

In this paper, a dry type hollow reactor with a rated voltage of 35 kV and a rated capacity of 1200 kvar is studied as an example. The main parameters of this reactor are shown in Table.1.

TABLE 1. Dry type hollow reactor nameplate value parameters

Parameter name	Parameter value	Parameter name	Parameter value
Rated capacity	35 kV	Rated frequency	50 Hz
Rated voltage	1200 kvar	Insulated level	F
Rated inductance	20 mH	Number of packages	3
Rated current	216 A	Coil number	12

Most of the dry type hollow reactor consists of three basic parts: star support, insulation support device and winding. Reactor windings are composed of multi-parallel branches with multiple envelopes, multiple layers, and multiple conductors in parallel. Conductor using small cross-section round aluminum wire, wire wrapped with a layer of insulating polyester film for turn-to-turn and layer-to-layer; encapsulation between the insulation support strip composed

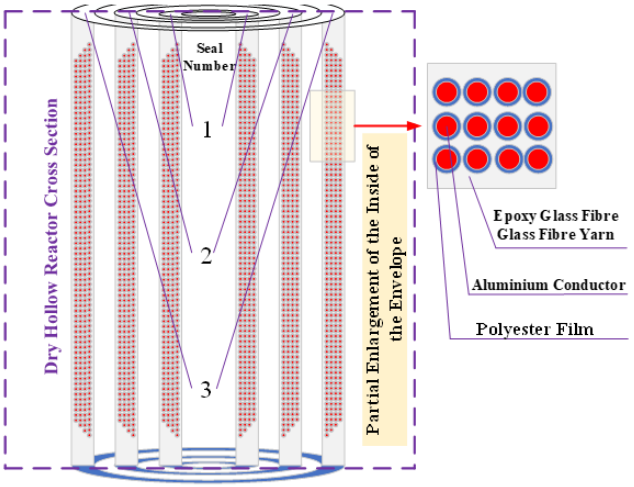

FIGURE 1. Structure of Dry Type Hollow Reactor.

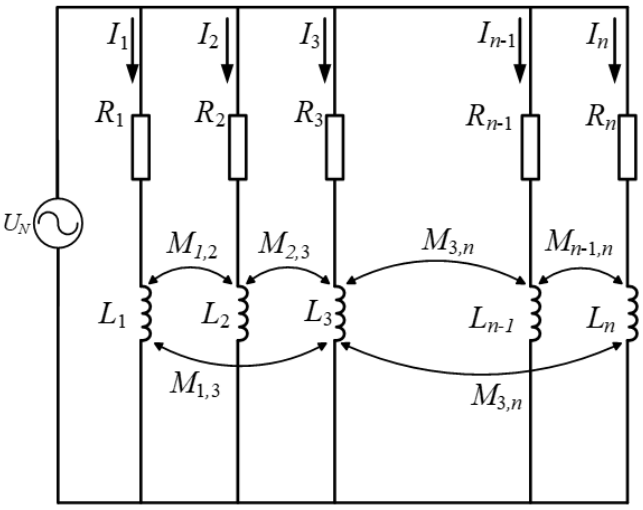

FIGURE 2. Reactor Equivalent Circuit Diagram.

of heat dissipation airway, its structure is shown in Fig.1. below.

The reactor as a whole is wound by three envelopes of twelve layers of aluminum conductors with wire diameter of $3\,\mathrm{mm} \sim 3.3\,\mathrm{mm}$ and envelope height of $694.8\,\mathrm{mm}$. The reactor is electrically a multi-coil parallel structure, helically wound by multi-layer aluminum conductors, with parallel connection between envelopes and layers, and parallel connection between layers.

Under normal operating conditions, the dry hollow reactor can be represented by a circuit model consisting of equal capacitance between turns and stray capacitance, equal resistance, and equal inductance. Due to the low-frequency state, the stray capacitance is small and the capacitive reactance is large, so the equivalent capacitance can be considered open-circuited, i.e., negligible. Therefore, the dry type hollow reactor can be simplified to a circuit composed only of inductance and resistance.

The dry hollow reactor adopts a coaxial parallel encapsulated structure. The equivalent circuit under normal operating conditions is shown in Fig.2. Assuming that the number of reactor encapsulation layers is n, and the self-inductance and frequency resistance of the i-th layer encapsulation are L_i and R_i, respectively. The mutual inductance between the i-th and j-th layers is denoted as M_{ij}.

$$\begin{cases} \sum_{j=1}^{n} j\omega M_{ij}\dot{I}_j + \dot{R}_i\dot{I}_i = \dot{U} \\ \sum_{i=1}^{n}\dot{I}_i = \dot{I} \\ \boldsymbol{M}_{ii} = L_i \end{cases} \tag{1}$$

The circuit equation is equation 1:

In equation (1), $\dot{U}$ is the loaded voltage across the reactor, in volts V; I is the total reactor current, in amperes A; I_i is the layer i encapsulation current, in amperes A; ω is the angular frequency, $\omega = 2\pi f$, where f is the system frequency, in hertz (Hz). The encapsulated self-inductance L_i and mutual inductance M_{ij} are obtained by finite element electromagnetic field calculations via the energy method.

B. COMPUTATIONAL MODELING FOR FINITE ELEMENT SIMULATION OF REACTORS

From Fig. 3 (a), it can be seen that the dry hollow reactor is a cylindrical symmetric structure, and the material parameters of each part are set the same, and the difference in the calculation results is relatively small, so in order to reduce the calculation time and the difficulty of the calculation, the authors take a quarter model of the reactor as the simulation object, as shown in Fig. 3 (b). In the calculation, the winding of each layer is taken as a unit, ignoring the influence of spacer, encapsulation and star bracket and other components on the electromagnetic field. The rated current calculation is a two-dimensional calculation, and the electromagnetic parameters are calculated with the current as the excitation, assuming that the coil current is uniformly distributed.

III. MATHEMATICAL MODEL

A. COMPUTATIONAL ANALYSIS OF FIELD-CIRCUIT COUPLING

The field-circuit coupling model is based on a finite element 1:1 computational model that simulation of its material properties and working environment. Calculating parameters such as self-inductance, mutual inductance and resistance of the reactor encapsulated coil, The coil current rating is then calculated from the equivalent circuit model. The magnetic field control equations are as follows.

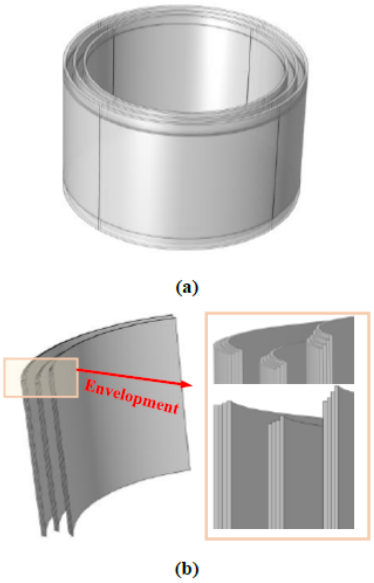

FIGURE 3. Finite Element Simulation Computational Modeling of Dry Hollow Reactor. (a) Reactor overall model and (b) Reactor 1/4 calculation model.

$$\begin{cases} \dfrac{\partial^2 A_\theta}{\partial r^2}+\dfrac{\partial A_\theta}{r\partial r}-\dfrac{A_\theta}{r^2}+\dfrac{\partial A_\theta}{\partial z^2}=-\mu J \\ \dfrac{\partial^2 A_\theta}{\partial r^2}+\dfrac{\partial A_\theta}{r\partial r}-\dfrac{A_\theta}{r^2}+\dfrac{\partial A_\theta}{\partial z^2}=0 \end{cases} \tag{2}$$

In equation (2), A_θ denotes the circumferential component of the vector magnetic potential $\mathbf{A}$; θ, z, and r represent the angular, axial, and radial coordinates in the cylindrical coordinate system, respectively; μ is the magnetic permeability of the aluminum conductor; and J denotes the current density in each layer of the winding.

B. COMPUTATIONAL ANALYSIS OF REACTOR FLOW-HEAT COUPLING

The reactor exchanges heat with the outside air in three forms: natural convection, radiation and heat conduction. The process of calculating the fluid-temperature coupling follows the fluid governing equations, i.e., mass conservation equation, momentum conservation equation, and energy conservation equation, in addition to satisfying the basic heat transfer equation [25]. The three-dimensional steady-state heat transfer equation for the reactor with the winding losses in each layer as the internal heat source is given by

$$\frac{\partial T}{\partial t}=\alpha\left(\frac{\partial^2 T}{\partial x^2}+\frac{\partial^2 T}{\partial y^2}+\frac{\partial^2 T}{\partial z^2}\right)+f \tag{3}$$

In equation (3), $\alpha = \frac{k}{c\rho}$, $f = \frac{F}{c\rho}$; T is the surface temperature of each layer of the winding; k is the coefficient of thermal conductivity; c is the specific heat capacity; ρ is the material density; and F is the heat source strength.

$$\rho\left(\frac{\partial u}{\partial x}+\frac{\partial v}{\partial y}+\frac{\partial w}{\partial z}\right)=0 \tag{4}$$

In equation (4), ρ is the air density; u, v, and w are the components of the fluid velocity vector along the x, y, and z coordinate axes, respectively. The momentum conservation equation is

$$\begin{aligned} \rho\frac{\mathrm{d}u}{\mathrm{d}t}&=\rho F_x+\frac{\partial \sigma_x}{\partial x}+\frac{\partial \tau_{yx}}{\partial y}+\frac{\partial \tau_{zx}}{\partial z} \\ \rho\frac{\mathrm{d}v}{\mathrm{d}t}&=\rho F_y+\frac{\partial \tau_{xy}}{\partial x}+\frac{\partial \sigma_y}{\partial y}+\frac{\partial \tau_{zy}}{\partial z} \\ \rho\frac{\mathrm{d}w}{\mathrm{d}t}&=\rho F_z+\frac{\partial \tau_{xz}}{\partial x}+\frac{\partial \tau_{yz}}{\partial y}+\frac{\partial \sigma_z}{\partial z} \end{aligned} \tag{5}$$

In equation (5), F is the body force; σ is the normal (positive) stress; and τ is the shear stress.

$$\rho\cdot\nabla(\boldsymbol{u}T)=\frac{\lambda}{c}+\nabla^2 T_f+S \tag{6}$$

In equation (6), $\mathbf{u}$ is the fluid velocity vector; T_f is the fluid temperature; λ is the air thermal conductivity; and S is the air viscous dissipation term.

C. MODEL CALIBRATION

The 2-dimensional simulation model of dry-type hollow reactor is established in maxwell computing software, and the vortex field is selected for solving, and the rated terminal voltage with the rated frequency of 50 Hz is applied at the ends of each layer of windings in the envelope to obtain the coil parameters of each layer; the coil current of each layer is obtained according to the field-circuit coupling calculation, and compared with the rated current. The calculation results are shown in the data in Table.2. below.

TABLE 2. Reactor Coil Simulation Rated Current Calculation

Envelopment	Floor	Field-circuit coupling resolution calculation value (A)	Rated current (A)	Error analysis (%)
1	1	21.27	21.35	0.37
	2	21.63	21.35	1.31
	3	21.89	21.35	2.53
	4	21.16	21.35	0.89
2	5	16.31	16.67	2.16
	6	16.27	16.67	2.40
	7	16.69	16.67	0.12
	8	17.01	16.67	2.04
3	9	16.34	16.12	1.36
	10	15.79	16.12	2.05
	11	16.21	16.12	0.56
	12	16.15	16.12	0.19

From Table.2. Reactor coil rated current simulation calculations: after applying the rated AC voltage to the two ends of the reactor, the maximum current flows through the 1, 2, 3 and 4 coils of the first layer of the encapsulated package. The difference in current values between the second and third wrapped coils is small. Comparing the reactor factory rated current, the maximum calculation error of the reactor coil is less than 4%, and the model calculation accuracy is high.

IV. ANALYSIS OF THE EFFECT OF CURRENT HARMONIC FREQUENCY TEMPERATURE RISE IN REACTOR COIL

A. ANALYSIS OF HARMONIC CURVES AT DIFFERENT FREQUENCIES OF REACTOR COIL CURRENT MIXING

Widely used non-linear load devices in power systems, such as electronic inverters, rectifiers, switching power supplies, etc., introduce many harmonics of the 3rd, 5th, 7th and

higher order. This paper uses the reactor field-circuit coupling calculation to obtain the coil rated current at industrial frequency, the first layer of the reactor coil current as an example, to study the influence of the industrial frequency fundamental current superimposed on different frequency harmonics on the current curve, the calculation formula is shown as follows.

$$I = I_N \sin(2\pi ft) + 0.35 I_N \sin(2\pi kf) \tag{7}$$

In equation (7), I is the coil current in amperes; I_N is the rated current, taken as 21.27 A; and k is the harmonic order. The results of the reactor coil current, mixing different frequency harmonic currents, are shown in Fig. 4 below.

As can be seen from the calculation of the reactor coil current curve in Fig.4.: As the frequency of the harmonic current increases, the degree of distortion of the total coil current waveform becomes more and more significant. The total current waveform amplitude relative to the fundamental waveform maximum increase of 34.97%, and with the increase in frequency, the total current amplitude change is not obvious, mainly because in order to quantitatively study the frequency increase on the electromagnetic parameters of the reactor operation, take the fundamental wave amplitude point of 0.05s, set the frequency increase step size of 1000Hz, so that the point with the increase in frequency to keep the same, the fundamental and harmonic currents are sinusoidal, if you take a fixed fundamental waveform After a certain point, with the increase of frequency, the harmonic waveform is close to the y-axis, and the total current amplitude always changes around the range of fundamental ± harmonic amplitude at that point. The degree of harmonic distortion is mainly manifested in the change of the number of peaks and valleys in the x-axis direction, the higher the frequency, the greater the number of peaks and valleys of the coil current.

B. ANALYSIS OF THE INFLUENCE OF THE MAGNETIC INDUCTION STRENGTH OF REACTORS WITH DIFFERENT HARMONIC FREQUENCIES OF FUNDAMENTAL CURRENT MIXING

In the geometrical analysis of the reactor, the dry hollow reactor can be regarded as an axisymmetric structure, ignoring the influence of spacers and star supports. Compared to the three-dimensional structure, the two-dimensional model cannot capture the overall electromagnetic field distribution of the reactor. However, it allows detailed modeling and calculation of each turn in each winding layer of the encapsulated winding, as shown in Fig.5(a).

From the curve calculation results in Fig.4, it can be seen that increasing the fixed frequency causes the fundamental amplitude to reach its maximum value (fundamental amplitude plus harmonic amplitude) multiple times.

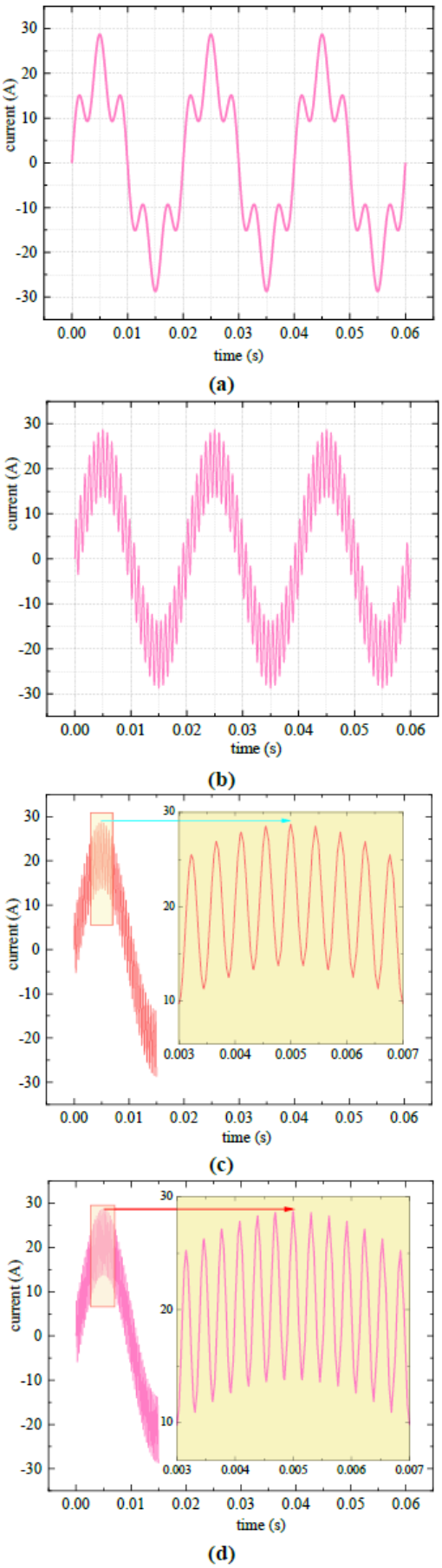

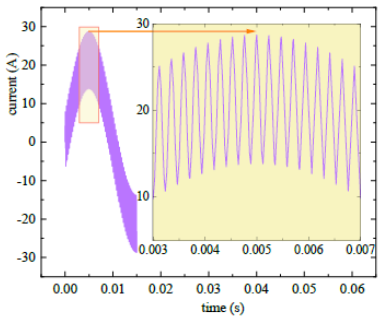

FIGURE 4. Reactor coil fundamental current mixed with different frequency harmonic curves. (a) $k = 5$ ($f = 250$ Hz); (b) $k = 25$ ($f = 1250$ Hz); (c) $k = 45$ ($f = 2250$ Hz); (d) $k = 65$ ($f = 3250$ Hz); (e) $k = 85$ ($f = 4250$ Hz).

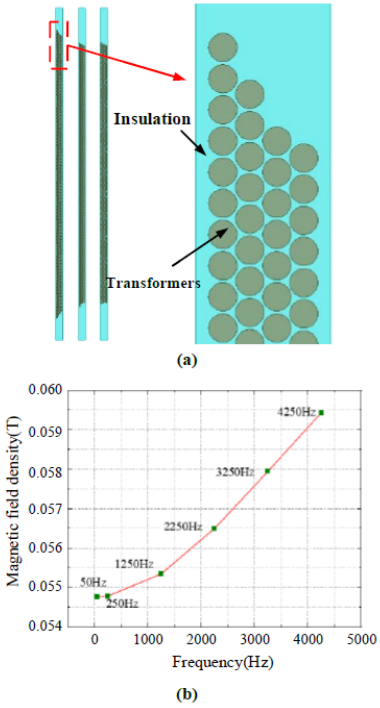

FIGURE 5. Finite element two-dimensional simulation model and electromagnetic field calculation results. (a) Finite element two-dimensional simulation models and (b) Maximum values of magnetic induction at different frequencies of the reactor.

Therefore, the harmonic superposition of the coil current in each layer of the encapsulated winding, calculated using Eq. (7), is used as the excitation source to simulate the maximum magnetic induction at different frequencies (from 50 to 4250 Hz), at the same moment (0.005 s) and with the same coil current amplitude. The simulation results are shown in Fig. 5(b).

From the calculation results in Fig.5. (b), it can be seen that with the increase of reactor coil frequency, the maximum magnetic induction intensity of the envelope is in an upward trend. The main reason is that the coil current frequency

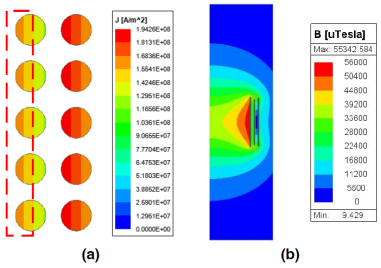

FIGURE 6. Frequency Variation of Magnetic Induction Strength and Coil Current Density Calculation Results for Reactor. (a) Current density distribution of the first layer coil and (b) 50 Hz Magnetic induction distribution.

increases, so that the magnetic induction intensity changes faster, the proximity effect between the coils is enhanced, the coil current is unchanged, resulting in the innermost coil near the center of the side of the current density enhancement, as shown in Fig.6. (a). So the magnetic field superposition at the center position of the innermost coil is enhanced and the maximum value of the magnetic induction strength is increased.

Since the magnetic field generated by the current at different frequencies are in accordance with the superposition theorem, the distribution of the magnetic induction intensity does not change much, and because the sinusoidal sources at different frequencies are analyzed, the cloud diagrams taken at the same time with the same current amplitude do not change significantly. In summary the distribution of magnetic induction at different frequencies is shown in Fig.6. (b).

C. SIMULATION AND CALCULATION OF FREQUENCY-ACTIVATED TEMPERATURE RISE OF DRY-TYPE AIR-CORE REACTORS

The temperature rise of the reactor is mainly calculated from the current obtained by field-circuit coupling, through harmonic superposition, its coil resistance loss, eddy current loss, circulating current loss, and finally in the form of volumetric heat source density for fluid-heat coupling simulation calculation. The reactor resistance is shown by the total coil losses as follows (8).

$$P_h+P_c+P_e=P_i \tag{8}$$

In equation (8), P_i is the coil loss at layer i, in watts (W).

The reactor resistance loss is:

$$P_h = \sum_{i=1}^{n} I_i^2 R_i \tag{9}$$

In equation (9), I_i is the effective value of the winding current at each level, in amperes (A). R_i is the DC resistance of each layer of the reactor, in ohms (Ω).

The envelope circulation loss is:

$$P_c = \sum_{i=1}^{n} (\dot{I}_i - \frac{\dot{I}}{n})(\dot{I}_i - \frac{\dot{I}}{n})^* R_i \tag{10}$$

Reactor encapsulated eddy current loss is:

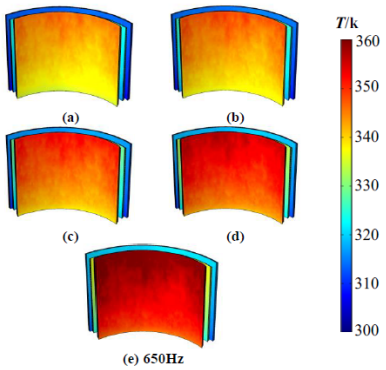

FIGURE 7. Distribution of reactor temperature rise under the effect of harmonic frequency. (a) 250Hz(Tmax=377K); (b) 350Hz(Tmax=380K); (c) 450Hz(Tmax=385K); (d) 550Hz(Tmax=392K) and (e) 650Hz(Tmax=400K).

$$P_e = \sum_{i=1}^{n}\sum_{j=1}^{k} \frac{D_i \pi^2 \omega^2 d_i^4}{64\rho} B^2 \tag{11}$$

In equation (11), k is the number of layers encapsulated, n is the number of turns corresponding to each layer of the encapsulation, D_i is the inner diameter of the wire, d_i is the wire diameter, and B is the magnitude of the magnetic induction intensity at the center outside the wire in the layer.

The heat source density is obtained by measuring the coil volume of each layer of the reactor package, ranging from 0.0059 to 0.0079 m^3, by dividing the loss by the volume. Using a fluid-heat coupling model, the finite element physical field simulation calculating the temperature rise distribution of the reactor is shown in Figure 7 below.

From the reactor temperature distribution calculation results shown in Fig.7, it can be observed that the reactor surface temperature gradually increases with the superposition of harmonic frequencies on the system reactor coil current. When the frequency increases from 250 Hz to 4250 Hz, the maximum temperature of the reactor rises from 377 K to 400 K, an increase of 6.1%.

According to equation (11), this temperature rise is mainly due to the increase in both the maximum magnetic induction strength B and the angular frequency ω, which results in higher eddy current losses. Based on the fluid-heat coupling principle, the heated air removes most of the heat from the bottom of the reactor, causing the temperature distribution on the reactor's encapsulated surface to exhibit higher temperatures at the top and lower temperatures at the bottom.

V. ANALYSIS OF THE EFFECT OF CURRENT HARMONIC CONTENT ON REACTOR TEMPERATURE RISE

A. ANALYSIS OF THE EFFECT OF MIXING DIFFERENT CONTENT OF HARMONIC CURRENT CURVES IN REACTOR COILS

In addition to the superimposed harmonics, the fundamental current of the power system also has different contents, so the reactor coil current superimposed with different contents

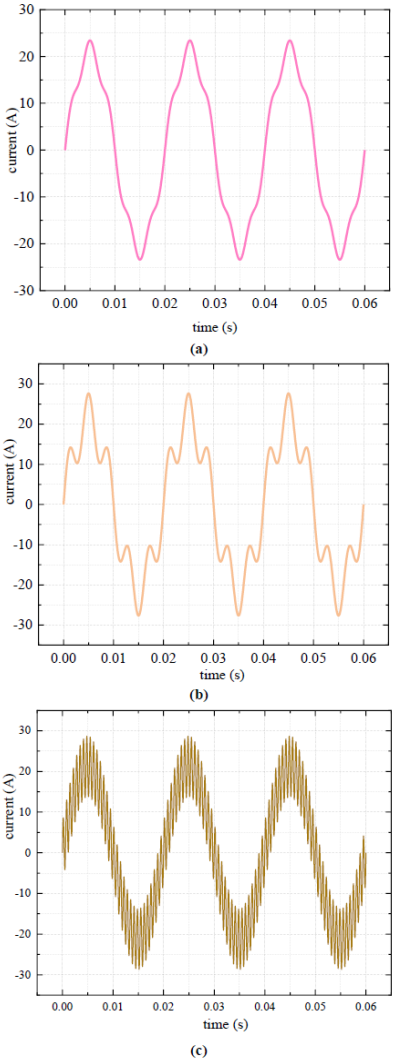

FIGURE 8. Reactor coil fundamental current mixed with different content of harmonic curves. (a) a=10%, (b) a=30% and (c) a=50%.

of harmonics is considered to be studied. The first layer of reactor coil is also used as an example, superimposed on the common 5th harmonic of the power system, to analyze the impact of harmonic content. The calculation formula is as follows equation (12)

$$I = I_N \sin(2\pi ft) + aI_N \sin(2k\pi f) \tag{12}$$

In equation (12), I is the coil current, in amperes (A); I_N is the rated current, in amperes (A); and k is the number of harmonics, where k is taken as 5. The results of the reactor coil fundamental current mixed with harmonics of different contents calculated by the above formula are shown in Fig. **??** below.

From Fig.8. The results of fundamental current mixed with different contents of harmonic calculation the reactor can be seen: with the increase of harmonic content, the current curve of the reactor coil distortion effect is significant, and the total current waveform amplitude also increases with the increase of harmonic content. Taking the 5th harmonic current as an

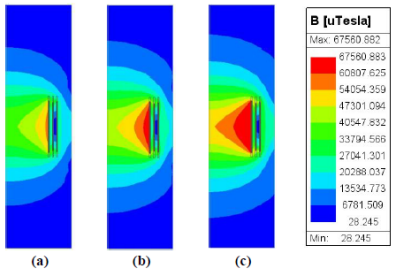

FIGURE 9. Distribution of magnetic induction strength for reactors with different harmonic content. (a) a=10%, (b) a=30% and (c) a=50%.

example, when the harmonic current content increases by 0% 60%, the total current peak value increases by 59.3%. The direction of distortion is mainly on the y-axis.

B. ANALYSIS OF THE INFLUENCE OF THE MAGNETIC INDUCTION STRENGTH OF REACTORS WITH DIFFERENT FREQUENCIES OF HARMONIC CONTENT MIXED WITH THE FUNDAMENTAL CURRENT

In the finite element calculation software, the harmonic content influence curve of coil obtained from the field and road coupling as current excitation, each layer of winding single-turn coil of the reactor applied, the material is applied, the attribute settings are the same as the harmonic frequency analysis, the time domain calculation. To each curve reaches the maximum value of the moment 0.005s, the reactor coil current superimposed on the different content of harmonic magnetic induction intensity distribution calculation results are shown in Fig.9.

From the Fig.9 above. Calculation results can be seen: With the increase of the reactor coil current superimposed harmonic current content of each layer, its surrounding magnetic induction intensity shows an increasing trend, when the harmonic current content increased from 10% to 60%, the maximum magnetic induction intensity from 0.057T to 0.083T, incresed by 45.61%, can be seen that the growth of the magnetic induction intensity and the instantaneous current amplitude excitation is almost directly proportional to the growth of the excitation. And as for each harmonic content, the magnetic field distribution of reactor is the same, presenting the first layer of encapsulation center position out of the magnetic induction intensity is the largest, the magnetic induction intensity reaches the maximum value, and the second and third layer of encapsulation compared with the difference is obvious, and the main reason is a layer of windings in the space of each place to produce the magnetic field superposition results.

C. ANALYSIS OF THE EFFECT OF TEMPERATURE RISE ON THE HARMONIC CONTENT OF REACTORS

In order to analyze the effect of the reactor coil superimposed current content on its temperature rise, the total reactor coil current I and magnetic induction intensity B obtained from the above calculations are used to calculate the total

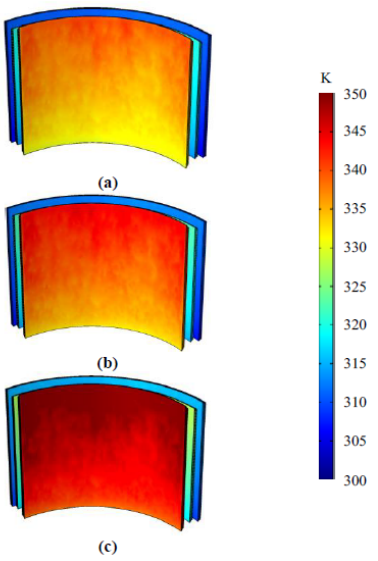

FIGURE 10. Calculation results of reactor temperature rise distribution under different harmonic contents. (a) a=10%, (b) a=30% and (c) a=50%.

coil loss according to Equations.(9) to (11). Each layer of coil loss divided by its volume to obtain the volume heat source density and finite element fluid-heat coupling calculations, obtained as shown in Fig.10. Reactor temperature rise distribution

The temperature rise calculation results of the reactor show that with the increase of different contents of superimposed harmonics, the temperature of all layers of the reactor encapsulation increases, and the maximum temperature of the encapsulated surface is maintained at about 350K, which does not exceed the temperature rise limit specified in the standard for this type of reactor. This is mainly due to the fact that with the increase of harmonic superposition content, the coil current amplitude rises, and the increase of current RMS indirectly causes the increase of magnetic induction intensity. By analyzing Equations (9) to (11), the coil resistance loss, circulating current loss, and coil current and eddy current loss are positively correlated with the magnetic induction intensity, and therefore, the encapsulation resistance, circulating current, and eddy current loss increase, and the same volume produces a higher heat source density. In order to respond more clearly to the harmonic content on the reactor temperature distribution , the reactor radial and axial temperature analysis, Figure.11. for different harmonic content of the reactor radial temperature part of the curve, Table.3. for the reactor axial position of the maximum temperature.

TABLE 3. Maximum radial temperature rise of the reactor

Harmonic content	Maximum temperature rise of the reactor (T/K)		
Axial position	$a = 10\%$	$a = 30\%$	$a = 50\%$
0.2	366.79	372.74	384.88
0	365.83	371.80	383.79
-0.2	365.12	371.03	382.95

From Fig. 11 radial temperature distribution curve and

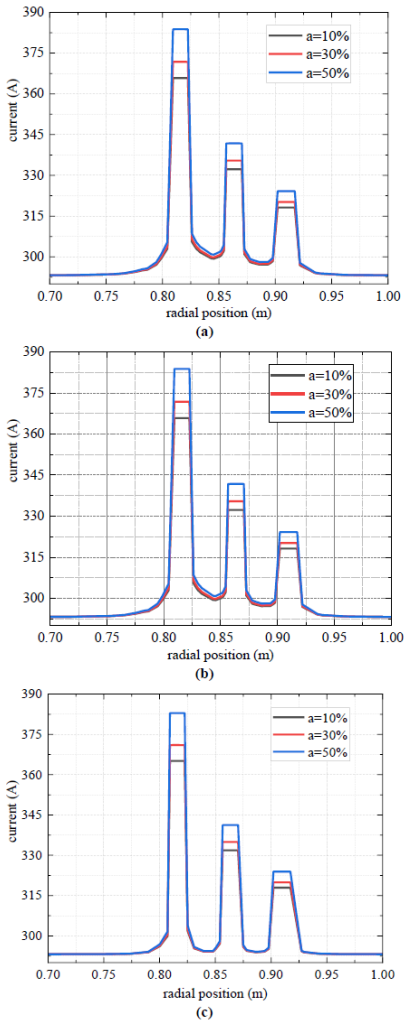

FIGURE 11. Radial temperature distribution of reactor under the effect of harmonic content. (a) Axial height 0.2, (b) Axial height 0 and (c) Axial height -0.2.

Table 3 of maximum reactor temperature, it can be observed that with the increase of coil current harmonic content, the internal temperature distribution of the reactor also shows an increasing trend. Compared with the envelope surface temperature, the internal temperature rise of the reactor is higher. When the harmonic current content increases to 50%, the temperature rises to 385 K, which does not exceed the corresponding F-class insulation temperature rise limit of 95 °C.

The internal and surface temperatures of the reactor coils exhibit the same trend with respect to the encapsulation position, decreasing from top to bottom ($z = 0.2\,\mathrm{m} \sim z = -0.2\,\mathrm{m}$), with the internal temperature decreasing slightly less than the external temperature. Overall, an increase in harmonic content inevitably causes an increase in the total current RMS, resulting in higher coil resistance losses and eddy current losses. However, the harmonic content of a power system generally rarely exceeds 35%, except when multiple frequency harmonics superimpose in the system, which may cause the total current RMS to increase and consequently lead to a temperature rise exceeding the allowable limit.

VI. DISCUSSION

A. SOURCES OF ERROR

Although the model was realistically constructed in the simulation of key reactor parameters and actual materials were parameterized, there remains a data error ranging from 0.19% to 2.53% in the validation of the coil current parameter calculation results. The main reason for this discrepancy is the limitation of physical field modeling in the finite element software used for simulation, which partially simplifies the reactor coil structure.

TABLE 4. Comparison of Simulated and Analyzed Resistance Values

Coil	Sim. (Ω)	Ana. (Ω)	Coil	Sim. (Ω)	Ana. (Ω)
1	2.07	2.09	7	1.79	1.81
2	2.05	2.07	8	1.79	1.80
3	2.03	2.04	9	1.49	1.52
4	2.02	2.03	10	1.49	1.52
5	1.81	1.82	11	1.49	1.52
6	1.79	1.81	12	1.50	1.53

For example, replacing the helical coil with a series of two-dimensional single-turns of wire, there is an error in the length of the coil, resulting in an inconsistency between the coil resistance and the resolved resistance, as shown in Fig. 3. This results in the inconsistency between the coil current and the rated current when the rated voltage is calculated. However, the accuracy of the reactor modeling is verified by the fact that the simulated resistance of the reactor coil at each layer is almost the same as the resolved value and through the calculation, the standard deviation of the coil current of each layer of envelope 1, 2 and 3 is 0.64, 0.20 and 0.08 respectively, which is a small deviation from the rated current, verifying the accuracy of the simulation modeling.

B. SIMULATION OF SEPARATE CALCULATIONS

Reactor temperature rise simulation loss and temperature rise using a separate calculation. Electromagnetic calculation process, need to consider the frequency change in the reactor coil single turn wire itself “skin effect” and turn-to-turn “eddy current effect” caused by the coil loss, can not be simplified coil, so this part of the reactor two-dimensional turn model for the Therefore, the two-dimensional turn model of reactor is used in this part for the field circuit calculation. In the fluid-heat coupling calculation of reactor temperature rise, only the reactor package winding temperature calculation and analysis, in order to determine whether the insulation temperature limit is exceeded. At this time, the volume heat source can be calculated by adding the coil turn losses of each layer, and the overall simplified model of the three-dimensional coil can be established. Under the premise of ensuring that the calculation is proficient, the simulation

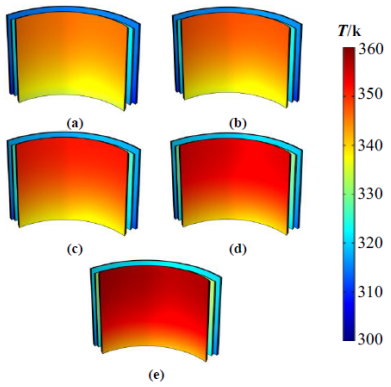

FIGURE 12. Verification of steady-state thermal temperature rise of reactors. (a) 250Hz; (b) 350Hz; (c) 450Hz; (d) 550Hz and (e) 650Hz.

steps can be reasonably simplified, which can improve the efficiency of the calculation and reduce the calculation time.

C. ARTICLE CONFIDENCE ANALYSIS

In order to increase the credibility of the multi-physics field calculation method of the electromagnetic-fluid-temperature field of the reactor, the steady state thermal method is used for simulation verification. The calculated coil resistance of each layer of the reactor and the volumetric heat source of each layer from the eddy current calculation loss are loaded into the steady-state solid heat transfer physical field, the same ambient temperature of 297.3 K is set, the surface ambient radiation is set on the encapsulated surface of the reactor, and the bottom of the coil is set as natural convection, and the results are solved and calculated as shown in Fig.12. Combining Fig. 7 and Fig. 12 with the cloud diagram of the temperature part of the reactor, it can be seen that the temperature field calculated by the multiphysics field coupling simulation method has the same distribution law as that calculated by the steady state thermal analysis method.

As can be seen from Table 5, the maximum temperature rise of the reactor calculated by electromagnetic-fluidic thermal coupling and steady state thermal analysis at different frequencies is extremely similar, which verifies the accuracy of the electromagnetic-fluidic thermal coupling calculation method for the reactor.

TABLE 5. Comparison of multi-physics field coupling and thermal steady-state calculated temperature rise

Methodologies Frequency (Hz)	Multiple Physical Field Coupling (K)	Thermal Steady-State Calculations (K)
250	377	375
1250	380	382
2250	385	386
3250	392	391
4250	400	396

VII. CONCLUSION

For the study of the temperature rise of harmonic high level contamination of dry hollow series reactor type products, it is proposed to establish a two-dimensional axisymmetric model considering the line-turn magnetic induction by means of the finite element simulation software COMSOL .In order to verify the correctness of the designed mathematical model of the reactor, its coil current is verified using field-circuit coupling calculations, and the calculation error is controlled within 3%. Compared with the overall modeling of the coil, the single-turn modeling takes into account the proximity effect between turns as well as the resistance loss due to its own skin effect. Simulation of the model shows that the content and frequency of harmonic currents affect the reactor coil current waveform to different degrees. The larger the harmonic current content and frequency, the more serious the wave form distortion of the reactor, and the higher the temperature rise In our future work, we will test the reactor of this type and model to verify the accuracy of the model, so as to make the experiment more rigorous and more convincing.

REFERENCES

[1] Y. Zou, J. X. Wang, J. Dai, Y. Zhou, et al. Impacts and Mitigation Measures of European Energy Crisis[J]. Automation of Electric Power Systems, 2023, 47(17):1-13.
[2] NEA releases national power industry statistics for 2022[J]. Electric Power Survey & Design, 2023(01):24.
[3] Y.B. Shu, G. P. Chen, J. B. He, et al. Building a New Electric Power System Based on New Energy Sources[J]. Building a New Electric Power System Based on New Energy Sources, 2021, 23(6):61-69.
[4] Y. H. Xu, C. F. Xue, S. Tao, et al. Review on harmonic power flow calculation method for power system[J]. Electrical Measurement & Instrumentation, 2023, 60(12):1-10.
[5] Y. H. Li, Y. Y. Sun, Q. Y. Wang, et al. Data-Driven Probabilistic Harmonic Power Flow Calculation Based on Source and Load Harmonic Coupling Model[J]. Proceedings of the CSEE:1-12 [2023-12-21 13:07].
[6] J. W. Li, B. Y. Wu, Y. G. Li, et al. Gray-box Wide Frequency Domain Matrix Model of Inverter for Harmonic Degradation Mechanism Analysis and Its Solution Method[J]. Automation of Electric Power Systems, 2020, 44(18):155-163.
[7] Ziegelberger G, Vecchia P, Hietanen M, et al. Guidelines on limits of exposure to static magnetic fields[J]. Health Physics, 2009, 96(4):504-514.
[8] S. J. Wang, D. P. Wu, G. X. Ma, et al. Abnormality Analysis of 750 kV High Voltage Shunt Reactor Through Partial Discharge Detection[J]. High Voltage Apparatus, 2023, 59(08):78-83+90.
[9] W. M. Zhang, W. Li, Y. L. Liu, et al. Analysis Cause Burn-out of 35 kV Dry-type Air-core Series Reactor[J]. Power Capacitor & Reactive Power Compensation, 2022, 43(05):57-63.
[10] Z. Y. Li, L. X. Wang, F. Liu, et al. Research on electromagnetic calculation and loss of the design of dry-type air core reactor by isothermal rise method[J]. Heilongjiang Electric Power, 2019, 41(05):421-428.
[11] Y. J. Zhang, W. N. Qin, W. J. Liu, et al. Ventilation Structure Improvement of Reactor Based on Coupled Field Numerical Analysis[J]. High Voltage Apparatus, 2014, 50(08):62-67.
[12] S. Y. Wu, H. Z. Ma, N. Jang, et al. Simulation and analysis of temperature field of high voltage reactor based on multi physical field coupling[J]. Power System Protection and Control, 2019, 47(04):17-24.
[13] L. Q. An, Z. Q. Wang, G. J. Tang. Three-dimensional temperature field finite element analysis and temperature rise experiment of dry reactor[J]. Journal of North China Electric Power University (Natural Science Edition), 2002, (03):75-78.
[14] X. L. Wei, "Theoretical studies related to the design and calculation of large dry hollow power reactors," Ph.D. dissertation, Dept. Elect. Eng., Harbin Institute of Technology, Harbin, China, 2002.

[15] H. X. Zhao. Fitting Algorithm of Mean Temperature Rise of Dry-Type Air-Core Reactor[J]. Transformer, 1999, (12):7-9.
[16] W. Jin, L. J. Fu, T. W. Xia. The Analysis of the Eddy Losses for Dry Type Air Cored Reactor[J]. Journal of Shenyang Ligong University, 1999, (03):79-82.
[17] T. W. Xia, Y. D. Cao, W. Jin, et al. The Analysis of Temperature Field in Dry Air Core Reactor[J]. High Voltage Engineering, 1999, (04):86-88.
[18] Z. G. Ye. Temperature Rise Test of Dry-Type Air-Core Reactor and Calculation of its Winding Temperature Rise[J]. Transformer, 1999, (09):6-12.
[19] L. S. Zeng, L. X. Zhang, D. X. Xie. Separation Calculation of Harmonic Loss of EHV Dry-Type Smoothing Reactor[J]. Transformer, 2011, 48(04):6-9.
[20] Qiu D, Zhenbiao Li, Xiaogen Y, et al. Steady Thermal Field Simulation of Forced Air-cooled Column-type Air-core Reactor[J]. High Voltage Engineering, 2013, 39(4):6.
[21] Burke P E. Effect of eddy losses on the design and modelling of air-cored reactors[J]. IEEE Transactions on Magnetics, 1991.
[22] Ram B S. Inductance and winding eddy loss of air-cored reactors[J]. IEE Proceedings Part C, 1999, 146(5):416-420.
[23] Kurita N, Onda K, Nakanoue K, et al. Loss Estimation Method for Three-Phase AC Reactors of Two Types of Structures Using Amorphous Wound Cores in 400-kVA UPS[J]. IEEE Transactions on Power Electronics, 2014, 29(7):3657-3668.
[24] Ortiz C, Skorek A, Lavoie M, et al. Parallel CFD Analysis of Conjugate Heat Transfer in a Dry Type Transformer[C]// Industry Applications Conference. IEEE, 2007.
[25] Z. P. Jang, X. S. Wen, Y. Wang, et al. Test and Coupling Calculation of Temperature Field for UHV Dry-Type Air-Core Smoothing Reactor[J]. Proceedings of the CSEE, 2015, 35(20):5344-5350.

WANWEI WANG was born in 1982 in Hubei Province, China. He is currently working in Dongguan Power Supply Bureau of Guangdong Power Grid Co., Ltd. His title is senior engineer. His research directions include power grid stability analysis, reactive power compensation and new energy access to the grid.

RAN ZHUO was born in 1986. He is currently working in Electric Power Research Institute of China Southern Power Grid, with the title of professor level senior engineer. His research directions include transformer equipment insulation state detection and diagnosis technology, environmental protection insulation gas application technology, new power equipment application and detection technology.

RONGFU ZHONG was born in 1988. He is currently working in Dongguan Power Supply Bureau of Guangdong Power Grid Co., Ltd. His title is senior engineer, and his research direction includes high voltage of power equipment.

ZHIMING HUANG was born in 1985. He is currently a senior engineer at the Electric Power Research Institute of China Southern Power Grid. His research interests include numerical modeling and simulation, transformer oil-paper bushings, and gas discharge mechanisms.

CHENGZHOU ZHANG was born in 1987. He is a senior engineer at Dongguan Power Supply Bureau of Guangdong Power Grid Co., Ltd. His research interests include the Department of Electric Power.

YAN LUO was born in 1991. He is a senior engineer at the Electric Power Research Institute of China Southern Power Grid. His research focuses on new technology development for substation equipment and safe operation of equipment.

JIEMING HUANG was born in 1978. He is a senior engineer at Dongguan Power Supply Bureau of Guangdong Power Grid Co., Ltd. His research interests include substation equipment piping.

MENG GAO was born in 1990. He is a senior engineer at the Electric Power Research Institute of China Southern Power Grid. His research focuses on intelligent perception technology and device development for power transformers.

QIULIN CHEN was born in 1993. He is a senior engineer at the Electric Power Research Institute of China Southern Power Grid. His research focuses on intelligent perception technology and device development for power transformers.

YUN ZHANG was born in 1991. He is a senior engineer. His research focuses on intelligent perception technology and device development for power transformers.